

Optical Characterization of Bio-analytes in an Aqueous Environment

M.Sc. Thesis

By

KALI MEENA



**DISCIPLINE OF PHYSICS
INDIAN INSTITUTE OF TECHNOLOGY INDORE**

JUNE 2023

Optical Characterization of Bio-analytes in an Aqueous Environment

A THESIS

*Submitted in partial fulfillment of the
requirements for the award of the degree
of*
Master of Science

by

KALI MEENA



DISCIPLINE OF PHYSICS
INDIAN INSTITUTE OF TECHNOLOGY INDORE
JUNE 2023



INDIAN INSTITUTE OF TECHNOLOGY INDORE

CANDIDATE'S DECLARATION

I hereby certify that the work which is being presented in the thesis entitled **Optimal Characterization Of Bio-analytes in an Aqueous Environment** in the partial fulfillment of the requirements for the award of the degree of **MASTER OF SCIENCE** and submitted in the **DISCIPLINE OF PHYSICS, Indian Institute of Technology Indore**, is an authentic record of my own work carried out during the time period from June 2022 to June 2023 under the supervision of Dr. Pankaj R. Sagdeo, Head, Department of Physics, and Dr. Sharad Gupta, Associate Professor, Department of Bioscience and Biomedical Engineering.

The matter presented in this thesis has not been submitted by me for the award of any other degree of this or any other institute.

Kali Meena

Signature of the student with date
(KALI MEENA)

This is to certify that the above statement made by the candidate is correct to the best of our knowledge.

Pankaj R. Sagdeo

Signature of the Supervisor of
M.Sc. thesis #1 (with date) 08.06.2023
(Dr. Pankaj R. Sagdeo)

Sharad Gupta

Signature of the Supervisor of
M.Sc. thesis #2 (with date)
(Dr. Sharad Gupta)

KALI MEENA has successfully given her M.Sc. The oral Examination was held on **6 June 2023**.

Pankaj R. Sagdeo

Signature(s) of Supervisor(s) of MSc thesis
Date: 08.06.2023

Mandana Natar

Convener, DPGC
Date: 8.6.2023

Signature of PSPC Member #1
Date: 08.06.2023

Kali Meena

Kali Meena
Signature of PSPC Member #2
Date: 08/06/23

DEDICATION

This thesis is dedicated to my family.

ACKNOWLEDGEMENTS

I am honored and grateful to have completed this MSc thesis, and I would like to express my appreciation to those who have supported me throughout this journey.

I would like to begin by thanking my supervisor, Dr. Pankaj R. Sagdeo, for his invaluable guidance, expert knowledge, and constant support throughout my research. His contributions, insights, and expertise have been invaluable in shaping my research and in helping me overcome various challenges. His assistance and encouragement have been invaluable to me throughout my academic journey. I would like to express my sincere gratitude to my co-supervisor, Dr. Sharad Gupta, for his unwavering and invaluable guidance, mentorship, and support throughout this project work. His vast knowledge, constructive feedback, and timely suggestions have been instrumental in shaping this thesis. He consistently challenged me to think critically, push beyond my limits, and strive for excellence in my research. I am grateful for his availability, patience, and support, even during challenging times. I am also thankful for his unwavering availability to answer my questions and concerns and time-to-time discussions, even during the busiest of times. Dr. Sharad Gupta has been an outstanding mentor, and I feel fortunate to have had the chance to work with him.

I am grateful to the Departmental Post Graduate Committee (DPGC) and the Head of the Department of Physics for offering me the opportunity to work independently and pursue my research interests. Their support during challenging and hard times has been invaluable to me, and I would like to express my appreciation for their unwavering assistance.

I would also like to express my gratitude to the faculty members and the Department of Physics staff for their assistance, guidance, and support throughout my academic program. Their knowledge and expertise have been invaluable in shaping my academic journey and in providing me with the resources and infrastructure to conduct my research. I would like to express my gratitude toward the faculty

members who have played a significant role in my academic journey. Their lectures and comments were inspiring, insightful and have contributed greatly to my development as a researcher and as a person. I am deeply appreciative of the valuable feedback they have provided, which has helped me in improving my work.

I would like to express my gratitude to SIC, for allowing me to use highly valuable instruments such as Raman spectroscopy and SEM. Their expertise and guidance were invaluable in helping me obtain accurate and reliable results for my research. I express my gratitude to Omkar Rambadey, Kailash Kumar, and Ritu Nain for their assistance in my experiments.

I would like to express my sincere appreciation to the Department of Physics and the Department of Biosciences and Biomedical Engineering, Indian Institute of Technology, Indore for their unwavering support and assistance throughout my MSc program. Their assistance with administrative matters and technical support has been invaluable in helping me conduct my research. I thank both departments for offering me the necessary resources and infrastructure to conduct my research. The department's supportive and stimulating academic environment played a crucial role in my academic and personal growth.

Additionally, I would like to express my deep appreciation to my fellow lab mates who have played a crucial role in making this project successful. I am so grateful to Dr. Sandeep Chaudhary for his invaluable assistance and guidance. I would like to extend my heartfelt gratitude to Miss Anusha Srivastava for always being there for me and for her unwavering assistance in my experiments. She has provided valuable assistance in planning my experiments. Moreover, I appreciate the support provided by Mr. Abhijeet Singh, Ms. Sampurna Dasgupta, and Ms. Priyanka Payal. Their contributions have been invaluable to my research, and I am deeply grateful to have had their assistance.

I would like to express my deep appreciation to my family members, classmates, and friends, who have been a constant source of love, support, and motivation throughout my research journey. Particularly, I

am thankful to my father and brother for their steady support throughout my career. Their encouragement and support have played a vital role in keeping me motivated and focused. I would like to express my heartfelt gratitude to my best friend Manish for his encouragement, and friendship throughout my academic journey. His constant belief in my abilities and his willingness to listen when things were tough have been priceless. My friends have been a great source of inspiration, and their countless hours of conceptualizing, discussions, and constructive feedback have enriched my research and made the journey more pleasant.

I am deeply grateful to everyone who has contributed to my academic journey, whether directly or indirectly. Your encouragement, guidance, and support have played a crucial role in shaping my research and enabling me to achieve my academic aspirations. I would like to extend my heartfelt thanks to all those who have been a part of my journey.

Kali Meena

Abstract

Urine is a valuable body fluid that can provide significant diagnostic information about a person's health. Since ancient times, urine samples have been analyzed for various diseases, with urine primarily composed of water, non-protein nitrogenous compounds such as urea, creatinine, and uric acid, as well as trace amounts of proteins, hormones, enzymes, bacteria, metabolites, and inorganic ions such as chloride, sodium, and potassium. By measuring the varying concentrations of these constituents, a wide range of disorders can be detected at an early stage, including kidney disorders, UTIs, liver diseases, diabetes, and cancers. However, current analytical methods require sample preparation steps, reagents, specialized training, and expensive equipment. Therefore, there is a need for a rapid, reliable, and inexpensive approach that does not require any special preparation.

Overcoming the limitations of traditional methods, optical techniques such as fluorescence spectroscopy, IR spectroscopy, UV-vis spectroscopy, and Raman spectroscopy have shown great potential for rapid urine analysis. Raman spectroscopy is often preferred over these optical spectroscopic techniques due to its high specificity, sensitivity, and ability to provide detailed molecular information without the need for sample labeling. Compared to other spectroscopic techniques, Raman spectroscopy provides more detailed information on the analyzed samples' molecular structure and chemical bonding.

However, the clinical applications of optical techniques are limited due to poor signal collection and lack of reproducibility in the measured signal intensities from the analytes present in body fluids. To address these limitations, improved optical signal detection strategies could be incorporated. The aim of this thesis is to investigate the use of optical spectroscopy to check disease manifestation in body through the quantitative determination of trace amounts of analytes present in urine using Surface-Enhanced Raman Spectroscopy (SERS).

TABLE OF CONTENTS

Abstract	v
LIST OF FIGURES	ix
LIST OF TABLES	xi
ABBREVIATIONS	xiii
NOMENCLATURE	xv
Chapter 1: Introduction	1-14
1.1 Body Fluids	1
1.1.2 Urine	2
1.1.2.1 History of Urine Analysis	2
1.1.2.2 Composition of urine	3
1.1.2.3 Urine as a diagnostic tool	4
1.2 Conventional Techniques Used in Urine Analysis and Limitations	5
1.3 Optical spectroscopy-based urine analysis	6
1.3.1 Basic Principle of optical spectroscopy	6
1.3.2 Raman spectroscopy	8
1.3.2.1 Limitations of conventional Raman spectroscopy	9
1.3.2.2 Variants of Raman Spectroscopy	10
1.4 Raman Spectroscopy-based Urine Analysis	13
1.5 Aim of the Thesis	14
Chapter 2: Materials and Methods	15-24
2.1 Materials	15
2.2 Synthesis of gold nanoparticles	15
2.3 Sample Preparation	16
2.4 Characterization Techniques	17
2.4.1 UV-Vis Absorbance Spectroscopy	18

2.4.2	Scanning Electron Microscope	19
2.4.3	Transmission Electron Microscope	20
2.4.4	Raman Spectroscopy	21
2.5	Quantitative Estimation of Analytes	22
Chapter 3: Results and Discussion		25-34
Chapter 4: Conclusion and Future Prospect		35-36
References		37

LIST OF FIGURES

- Figure 1.1** Schematic representation of components of urine.
- Figure 1.2** A representation of the interaction between light and matter
- Figure 1.3** Raman scattering process during light-matter interaction
- Figure 1.4** Energy level diagram for scattering process where ν_i is incident light's frequency, ν_s is scattered light's frequency, $\Delta\nu$ is Raman shift, and h is plank's constant.
- Figure 1.5** The basic mechanism of the SERS; localized surface plasmon resonance of metallic nanoparticles, and the enhanced Raman signal of adsorbed analytes.
- Figure 1.6** Mechanism of NTERS technique: nano-aggregates formation and NTERS measurements.
- Figure 1.7** Mechanism of Drop Coating Deposition; Drop evaporation, and coffee ring formation of the aqueous solution.
- Figure 2.1** Synthesis of Gold Nanoparticles (Colorless to wine-red color)
- Figure 2.2** Schematic representation of absorption spectroscopy set-up
- Figure 2.3** Scanning Electron Microscope (SEM)
- Figure 2.4** Ray diagram of Transmission Electron Microscope (TEM)
- Figure 2.5** Raman instrumentation where the expanded form is ADL-achromatic doublet lens; LCF- laser clean-up filter; DM-dichroic mirror; M- plane mirror; OL- objective lens; NF- notch filter; CCD- charge-coupled device
- Figure 3.1** UV-vis absorbance spectrum of the synthesized GNPs
- Figure 3.2** (a) Scanning Electron Microscope (SEM) and (b) Transmission Electron Microscope (TEM) image of GNPs
- Figure 3.3** (a) Liquid Drop and (b) Dried drop containing GNPs and analyte
- Figure 3.4** The Raman spectrum of urea at 50 mM concentrations measured from the dried-up liquid drop.
- Figure 3.5** Raman spectrum of urea at 997 cm^{-1}

- Figure 3.6** The Raman spectrum of uric acid at 2.0 mM concentrations measured from the dried-up liquid drop.
- Figure 3.7** Raman spectrum of uric acid at 495 cm^{-1}
- Figure 3.8** The Raman spectrum of creatinine at 2.0 mM concentrations measured from the dried-up liquid drop.
- Figure 3.9** Raman spectra for creatinine at the different known concentrations at 683 cm^{-1}
- Figure 3.10** Calibration curve depicting the relationship between the Raman peak intensity and the concentrations of urea
- Figure 3.11** Correlation between Raman Intensity and Uric Acid Concentrations
- Figure 3.12** Calibration Curve Analysis for Creatinine Concentrations
- Figure 3.13** SERS spectrum of the unknown concentration of urea
- Figure 3.14** SERS spectrum of the unknown concentration of uric acid
- Figure 3.15** SERS spectrum of the unknown concentration of creatinine

LIST OF TABLES

Table 2.1: Different Urea Concentrations in Prepared Samples

Table 2.2: Varying Concentrations of uric acid for Analysis

Table 2.3: Prepared different concentrations of creatinine

ABBREVIATIONS

mM	Millimolar
Mg	Milligram
dL	Deciliter
A	Absorbance
I_T	Transmitted intensity
I_0	Incident intensity
ϵ	Absorption coefficient
D	Path length (in cm)
C	The concentration of the solution (in Molar)
μL	Microliter
h	Plank's constant ($h=6.626 \times 10^{-34}$ J.S)
$\Delta\nu$	Raman Shift (in cm^{-1})
ν_i	Incident light's frequency
ν_s	Scattered light's frequency
λ	Wavelength (in nm)

NOMENCLATURE

Mass spectrometry	MS
High-performance liquid chromatography	HPLC
Gas chromatography-mass spectrometry	GC-MS
Liquid chromatography-mass spectrometry	LC-MS
Surface-Enhanced Raman Spectroscopy	SERS
Nano-Trap Enhanced Raman Spectroscopy	NTERS
Drop-Coating Deposition Raman spectroscopy	DCDRS
Chloroauric Acid	$(\text{HAuCl}_4 \cdot 3\text{H}_2\text{O})$
Tri-Sodium Citrate	$(\text{Na}_3\text{C}_6\text{H}_5\text{O}_7 \cdot 3\text{H}_2\text{O})$
Gold Nanoparticles	GNPs
Scanning Electron Microscope	SEM
Transmission Electron Microscope	TEM
Ultraviolet-Visible	UV-Vis
Photo Multiplier Tube	PMT
Band Pass Filter	BPF
Dichroic Mirror	DM
Objective Lens	OL
Laser Clean-up Filter	LCF
Achromatic Doublet Lens	ADL
Notch Filter	NF

Chapter 1

Introduction

Accurate and rapid disease diagnosis is essential for effective disease management, proper treatment, and successful therapy. An early diagnosis can result in better treatment and early disease management [1, 2]. A proper diagnosis may involve a number of tests and evaluations for a number of health conditions, which can be difficult to diagnose. To make a diagnosis in these situations, doctors may combine several procedures such as laboratory tests, imaging examinations, and genetic testing.

Nowadays, various biological samples such as blood, urine, stool, etc. are commonly used to monitor a patient's health status and disease diagnosis. Biological samples employed in disease diagnosis are either solid or liquid. The majority of solid samples are made-up of tissues, feces, and mucus from the throat, nose, and genital area, while liquid samples contain various body fluids like blood, sputum, urine, and more [3, 4]. All these samples have different diagnostic significance. For large-scale health monitoring, liquid samples are chosen since they can be obtained more quickly.

1.1 Body Fluid

Body fluids refer to the fluids produced by the body, and they play a significant role in indicating the presence of disease. Changes in the concentration of specific components or biomolecules within biofluids can serve as indicators of certain diseases [5]. Detecting and quantifying these biomolecules at an early stage can enhance the survival rate of patients. Biofluids are highly suitable for diagnostic purposes due to their ease of collection, cost-effectiveness, and frequent use in clinical biology. Physicians often recommend biofluid analyses to patients as a means of diagnosing the persistence or progression of diseases. The collection of biofluids is considered relatively safe and minimally invasive, making them an ideal diagnostic tool.

Blood and its components, saliva, urine, tears, and sweat are the main body fluids. Some are already frequently used for disease diagnosis in clinical settings. Among these biofluids, urine is one such biofluid that can be collected in a painless manner and in large quantities. Urine contains information about the health status of a human being. Particularly, it can provide information about Kidney health.

1.1.2 Urine

Urine is a liquid waste product that passes through the urinary system before being expelled from the body. The blood is filtered by the kidneys to remove waste materials and extra fluid, which are then expelled as urine. The average person produces about 1-2 liters of urine each day, although this might vary depending on many factors like fluid intake, exercise, and certain medical problems [6]. Urine color might reveal important details about a person's general health.

The presence of various substances in the urine, such as proteins, glucose, can be indicative of certain medical conditions. As an example, kidney disease may be indicated by the presence of protein in the urine, whereas diabetes may be indicated by the presence of glucose. Analysis of urine can be used to diagnose a variety of medical conditions, such as urinary tract infections, kidney disease, liver disease, gout, etc. [7, 8]. Urine can be collected in a painless manner and in large quantities. Urine contains information about the health status of a human being. Particularly, it can provide information about Kidney health.

1.1.2.1 History of Urine Analysis

Human urine analysis, known as uroscopy before the 17th century and now known as urinalysis, was the first laboratory medicine technique completed more than 6000 years ago [9, 10]. From the start around 4,000 B.C., historic Babylonian and Sumerian physicians recorded their analyses of urine on clay tablets [11]. It was noticed in Hindu culture that some people's urine tasted sweet and that black ants were drawn to the sweet urine, a medical symptom found that is called diabetes nowadays [11]. Hippocrates states in his book Aphorisma that

bubbles on the outer layer of fresh urine are a sign of longer-term renal disease. Proteinuria is often the cause of surface bubbles in the urine, which may also be a sign of renal disease or an infection of the urinary tract [9].

1.1.2.2 Composition of Urine

Urine is a waste product that is produced by the kidneys as they filter excess water, electrolytes, and other waste products from the blood. More than 95% of urine is made up of water, while the remainder is made up of proteins, hormones, enzymes, bacteria, metabolites, and certain inorganic ions like chloride, sodium, potassium, calcium, magnesium, sulfate, and so on [12, 13]. Urine also contains a few nonprotein nitrogenous substances such as urea, creatinine, and uric acid.

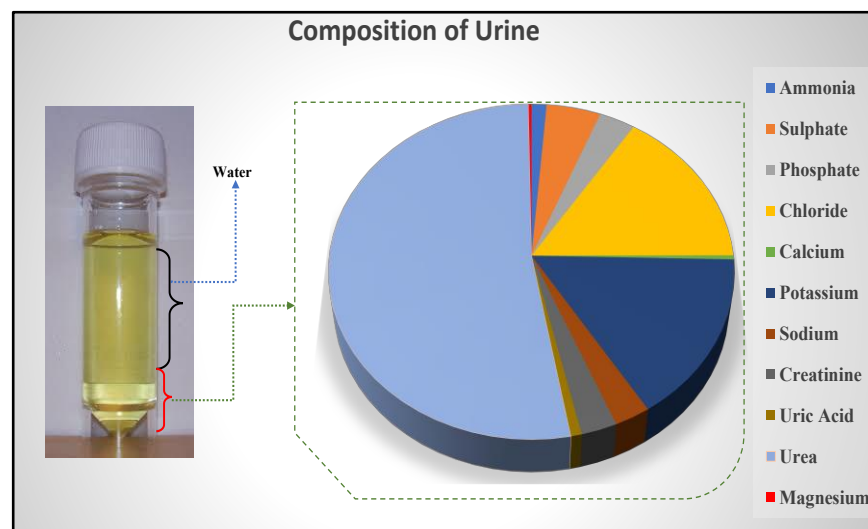


Fig. 1.1: Schematic diagram of components of urine

The concentration of these solutes in urine can vary depending on various factors such as diet, hydration status as well as their living and working environments. For example, a diet high in protein can increase the levels of urea and organic acids in urine, while dehydration can lead to increased concentrations of solutes such as sodium and potassium. The composition of urine can also be affected by various diseases and conditions, leading to changes in the levels of specific biomarkers and solutes.

1.1.2.3 Urine as a diagnostic tool

Urine can be used as a diagnostic tool to determine the stage of illness based on the changes in the concentration of a certain component or biomolecule. Urine is a by-product of kidney metabolism and is excreted from the body as waste. Urea, uric acid, and creatinine are important chemical biomarkers used to assess the health of the kidneys.

Urea is a waste product of protein metabolism that is typically excreted by the kidneys, while uric acid is a by-product of purine metabolism, and creatinine is a by-product of muscle metabolism. All three of these chemicals can be measured in the blood and urine and their levels can indicate the presence of kidney diseases or other health issues [14, 15].

The varying concentration of these biomolecules in urine might indicate uremia, gout, muscle diseases, metabolic disorder, dehydration, kidney failure, and kidney stones [16]. Doctors advise performing a urinalysis as part of a general physical checkup, during pregnancy, as a pre-surgery measurement, or to diagnose conditions like renal disease, diabetes, high blood pressure, and liver disorders. Many other symptoms, including backache, difficulty in urination, abdominal pain, and blood in the urine, call for a urinalysis. Therefore, quantifying urea, uric acid, and creatinine in urine is essential for identifying many disease states.

1.2 Conventional Techniques Used in Urine Analysis

In today's medical practice, chemical methods are used to do a quantitative urine analysis. These methods are different types of mass spectroscopy (MS), high-performance liquid chromatography (HPLC), gas chromatography-mass spectrometry (GC/MS), and liquid chromatography-mass spectrometry (LC/MS), etc. [17-23]. Mass spectrometry is a common analytical method for profiling urinary compounds. HPLC technique is used to identify and quantify urinary metabolites.

While these analytical methods have numerous advantages, they also come with some drawbacks. The sample processing steps in these methods are intensive in terms of chemicals, and preparing samples is a time-consuming process that requires multiple reagents and a specialized person for sample processing. Additionally, all these methods require the use of sophisticated, large, and costly apparatus for urinalysis. Further, due to the presence of other compounds, these methods are inclined to have errors due to interference, making them less specific. Other than this, urine samples can become contaminated with bacteria or other materials if kept for a long time which can interfere with the accuracy of the results.

Therefore, there is a need for an alternative approach that would provide inexpensive, rapid, and reliable urine analysis. This goal can be achieved by using optical characterization techniques for urine analysis. The commonly used optical characterization techniques are absorption, fluorescence, scattering, Raman spectroscopy, etc. Among all these methods Raman spectroscopy stands out because it can provide us with the fingerprint information of each analyte.

1.3 Optical spectroscopy-based urine analysis

Optical spectroscopy is a highly effective method employed for investigating the interaction between light and matter. It involves examining the characteristics of materials using electromagnetic radiation in the visible, ultraviolet, and near-infrared ranges. Techniques based on optical spectroscopy are currently showing great potential for urinalysis [24]. These methods can correlate particular biochemical changes of urine-based analytes to both their healthy and diseased states. These approaches are efficient analytical tools for monitoring human health because of their straightforward apparatus, low cost, and molecular sensitivity [25, 26].

1.3.1 Basic Principle of optical spectroscopy

According to the optical spectroscopy principle, when electromagnetic radiation interacts with matter, there can be a variety

of phenomena, such as absorbance, reflection, emission, scattering, or transmission, it depends on the characteristics of matter [27].

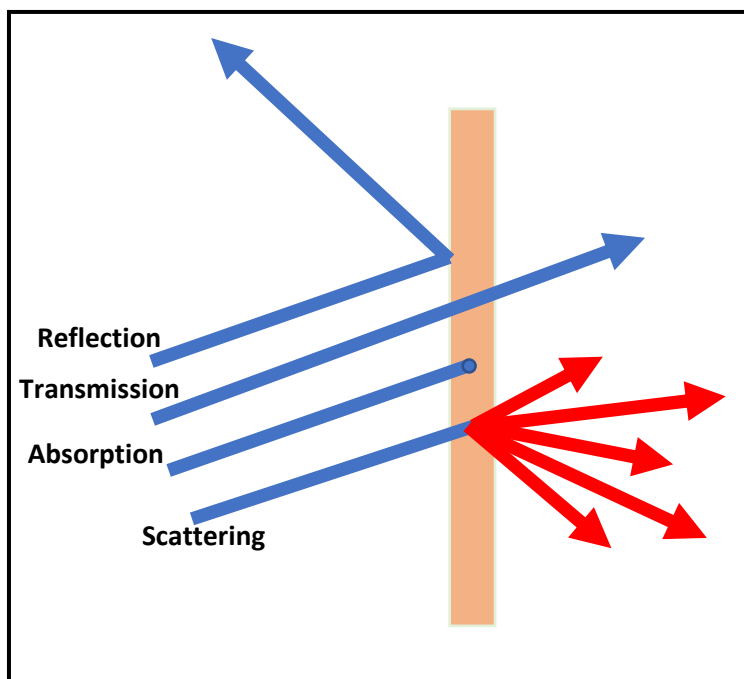


Fig. 1.2: A representation of the interaction between light and matter

The material's electrical and molecular structure determines how the radiation interacts with the matter (sample). The energy levels of the electrons or molecules within an object change when electromagnetic radiation interacts with them. This change may cause the emission or absorption of light at particular wavelengths, which can be detected and analyzed to reveal details about the material's characteristics.

There are several variants of optical spectroscopy that can be used for urine analysis, including fluorescence spectroscopy, UV-visible absorbance spectroscopy, and Raman spectroscopy.

Fluorescence spectroscopy is an optical method that enables the measurement of a sample's fluorescent characteristics without causing any damage to the sample. The main principle behind fluorescence spectroscopy is that when a sample is excited with a specific wavelength of light, it absorbs the energy and then emits light at a longer wavelength. This process is known as fluorescence and the emitted light is measured using a spectrometer. The amount and nature of the emitted light provide valuable information about the sample, including its chemical composition, molecular structure, and

concentration. Fluorescence spectroscopy is widely used in various fields of research, including biochemistry, medicine, and environmental sciences [28].

UV-visible absorbance spectroscopy is an influential analytical method employed to investigate the light absorption behavior of molecules within the ultraviolet and visible regions of the electromagnetic spectrum. This technique finds extensive applications across multiple disciplines such as chemistry, biochemistry, environmental science, and materials science, owing to its ease of use, high sensitivity, and non-invasive nature [29].

Raman spectroscopy is a non-invasive and non-destructive method that involves the scattering of light by molecules. It offers a distinct vibrational pattern characteristic of the molecules present in the sample, enabling the detection and measurement of different analytes in urine samples. Raman spectroscopy provides notable advantages, including its high specificity and sensitivity, making it an invaluable technique for urine analysis [30].

Raman spectroscopy is often preferred over these optical spectroscopic techniques due to its high specificity, sensitivity, and ability to provide detailed molecular information without the need for sample labeling. It also offers better resolution and is less susceptible to interference from water and other solvents. Compared to other spectroscopic techniques, Raman spectroscopy offers enhanced insights into the molecular structure and chemical bonds of the analyzed samples, providing a more comprehensive understanding of their composition [31].

1.3.2 Raman Spectroscopy

Raman spectroscopy is an effective analytical technique employed for the identification and characterization of the vibrational modes exhibited by various materials. It relies on the phenomenon of inelastic scattering, known as the Raman effect, which was first observed by C.V. Raman in 1928. In Raman spectroscopy, a focused laser beam with a specific wavelength is utilized as the light source [30, 31].

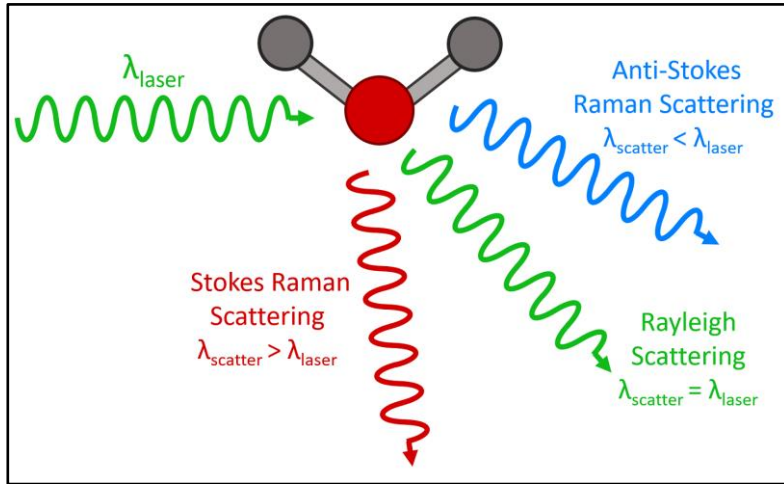


Fig. 1.3: Raman scattering process during light-matter interaction

When light interacts with molecules in a sample, the majority of photons scatter with the same energy as the incident photons, a phenomenon known as Rayleigh scattering or elastic scattering. However, a small fraction of photons undergo inelastic scattering or Raman scattering, where their energy levels differ from the incident photons. This scattering can result in scattered photons with frequencies higher ($\nu_i + \nu_s$) or lower ($\nu_i - \nu_s$) than the incident photons, referred to as anti-Stokes and Stokes scattering, respectively.

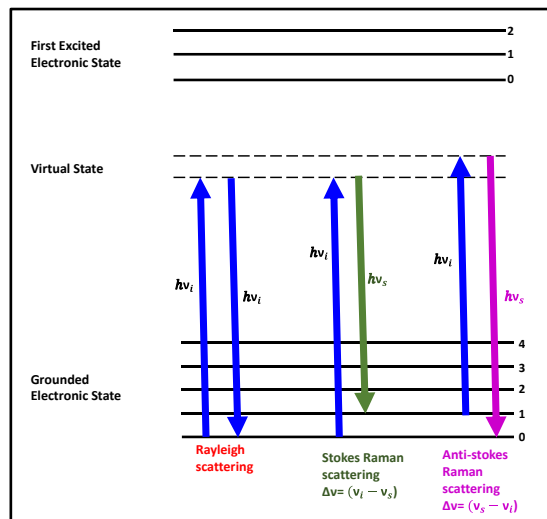


Fig. 1.4: Energy level diagram for scattering process where ν_i is incident light's frequency, ν_s is scattered light's frequency, $\Delta\nu$ is Raman shift, and h is plank's constant

A sample's Raman spectrum is obtained by observing the intensity of the scattered light as a function of the Raman shift. Many vibrational modes of the sample are represented as peaks in the spectrum. These

peaks can be identified by their location, magnitude, and shape, which can provide details about the sample's chemical structure, molecular bonds, and electronic configuration. Raman spectroscopy is used to produce a structural fingerprint of molecules that can be used to identify them. This non-invasive technique has been widely utilized in chemistry, materials science, biology, pharmacology, engineering, and among other fields.

1.3.2.1 Limitation of conventional Raman Spectroscopy

The Raman technique also has the advantage of being non-fatal and quick, requiring little or no sample preparation. The range of conventional Raman spectroscopy is limited because Raman signatures from urea, uric acid, and creatinine are relatively weak and we cannot get satisfactory results for low concentrations. It is challenging to measure low concentrations of a sample due to the weak Raman effect, which also leads to low sensitivity. This can be boosted by using one of the alternate techniques.

1.3.2.2 Variants of Raman spectroscopy

There are several variants of Raman spectroscopy, each with its own strengths. The need for these variants arises from the fact that different types of samples and applications require different types of Raman spectroscopy techniques to obtain the most useful and accurate results. Some of the main variants of Raman spectroscopy are as follows:

- **Surface Enhanced Raman Spectroscopy**

Surface-enhanced Raman spectroscopy (SERS) is a surface-sensitive method that is used to detect and characterize small molecules, biomolecules, and even individual molecules. It relies on the amplification of Raman scattering signals when molecules are adsorbed onto a roughened metal surface, leading to an augmentation in the Raman scattering cross-section. The level of enhancement is influenced by factors such as the size, shape, and composition of the nanoparticles, the excitation wavelength used, and the distance between the molecule and the surface [32, 33].

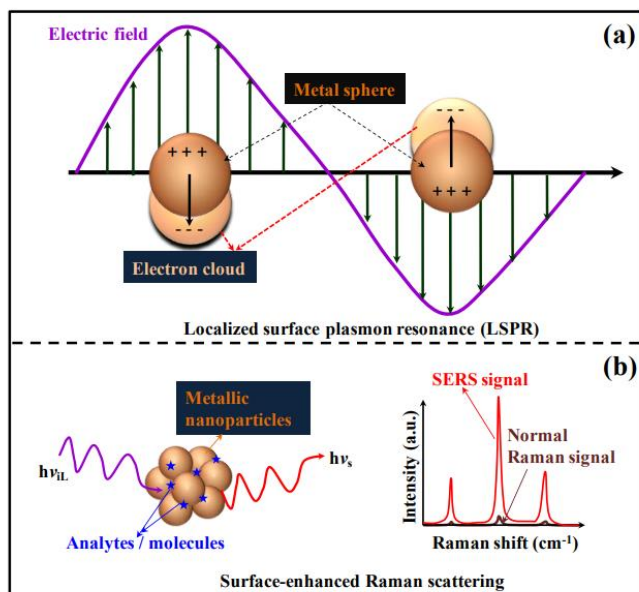


Fig. 1.5: The basic mechanism of the SERS technique, (a) localized surface plasmon resonance of metallic nanoparticles and (b) the enhanced Raman signal of adsorbed analytes [26].

There are two main mechanisms that are responsible for the enhancement of Raman scattering in SERS: the electromagnetic (EM) mechanism and the chemical mechanism.

The **electromagnetic mechanism** in surface-enhanced Raman spectroscopy (SERS) is based on the interaction between the incident electromagnetic field and the surface plasmons of metal nanostructures. When light interacts with metal nanoparticles, the conduction electrons within the metal can be collectively excited and oscillate, generating a resonance known as surface plasmon resonance. This phenomenon leads to a significant enhancement of the local electromagnetic field in the vicinity of the nanoparticles, creating specific regions called "hot spots." These hot spots greatly amplify the Raman scattering signals of molecules located nearby [34].

Chemical enhancement in surface-enhanced Raman spectroscopy (SERS) occurs when a molecule interacts with a metal surface. This interaction induces charge transfer between the molecule and the metal, causing alterations in the molecule's electronic structure. These changes have a direct impact on the Raman scattering cross-section of the molecule, resulting in the amplification of the Raman signal [35].

- **Nano-trap-enhanced Raman Spectroscopy**

Nano-trap-enhanced Raman spectroscopy (NTERS) is a modern approach used in Raman spectroscopy that offers the benefit of capturing and localizing molecules within a much smaller area compared to other Raman techniques. This method allows for more precise analysis of biological samples and enables the detection of even trace amounts of analytes in samples. To create hotspots for analysis, a microvolume drop containing a specific concentration of gold nanoparticles and bio-analyte is dried using a focused laser beam. The Raman spectra of these spots are then examined, and the Raman signal obtained from the analytes confined within the nanoparticle aggregates [36].

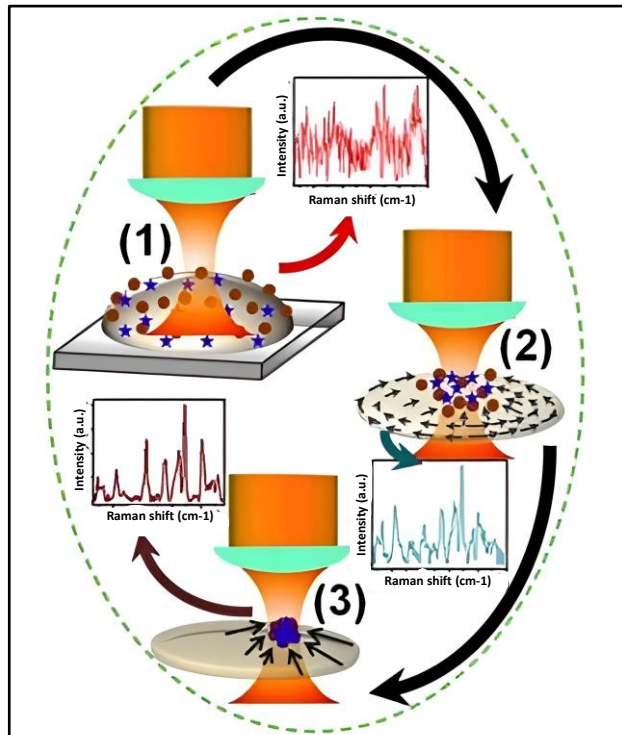


Fig. 1.6: Mechanism of NTERS technique: nano-aggregates formation and NTERS measurements [26].

When the laser is directed onto the nanoparticles, two forces are created: (a) gradient force and (b) scattering force. Gradient force pulls the particle towards the beam's focus and a scattering force pulls it along the beam's propagation path. By choosing a laser wavelength outside the nanoparticle's absorption band, the gradient force can trap the particle near the laser's focus, resulting in the formation of

nanoparticle clusters. Raman spectra can then be obtained from these areas to detect signals from the analytes localized within the nanoparticle aggregates.

- **Drop-coating deposition Raman spectroscopy**

Drop-coating deposition Raman spectroscopy (DCDRS) is an analytical method that merges the sensitivity of Raman spectroscopy with the flexibility of the drop-coating deposition technique. This technique relies on the drying process of a droplet on a solid surface, which leads to the formation of a distinctive pattern called a "coffee ring." As the droplet evaporates, non-volatile solutes are left behind, resulting in a concentrated distribution of suspended particles [37].

During the evaporation process, the fluid flux of the drop is driven by surface tension towards the edge of the droplet, and the movement of suspended particles to the edge leads to the formation of the coffee ring pattern.

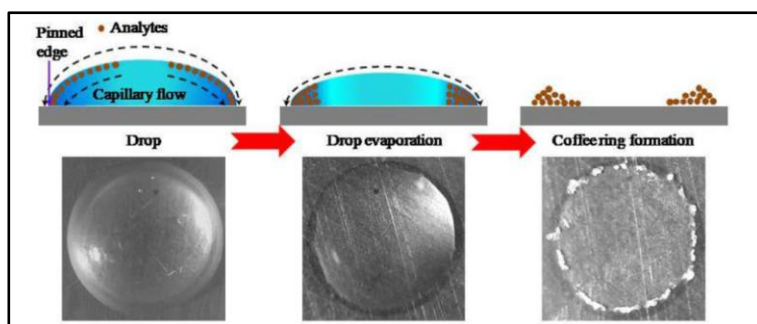


Fig. 1.7: Mechanism of Drop Coating Deposition; Drop evaporation, and coffee ring formation of the aqueous solution.

The DCDRS technique involves the deposition of a small volume of solution onto the dried solid substrate. The Raman spectrum of the deposited film is then measured using a Raman spectrometer equipped with a microscope. The resulting Raman spectra provide information on the molecular structure and composition of the deposited film [38].

1.4 Raman Spectroscopy-based Urine analysis

In recent years, Raman spectroscopy has emerged as a valuable technique for urine analysis. It offers a robust method for investigating the chemical composition of urine, allowing the identification and quantification of specific compounds or molecules within the sample.

Its chemical specificity makes it particularly well-suited for the precise detection of urinary biofluids, enabling the measurement of even subtle changes in the concentration of chemical components. Raman spectroscopy has proven effective in the identification and quantification of nitrogenous compounds like urea, creatinine, uric acid, and others, showcasing its utility in urine analysis.

Premasiri et al. were the first who demonstrated the application of Raman spectroscopy for urine analysis. They investigated the use of both traditional Raman spectroscopy and surface-enhanced Raman spectroscopy (SERS) for this purpose [24]. Since then, numerous studies have been conducted to explore the potential of Raman spectroscopy for disease detection using urine samples. For instance, Elzo E. et al. employed Raman spectroscopy to analyze urine samples from diabetic and hypertensive patients without renal disease [39]. Canetta et al. utilized Raman spectroscopy to detect bladder tumor cells in urine samples [40]. Holly J Butler et al., characterized biological molecules using Raman spectroscopy. Teodoru Soare et al. identified uric acid accumulation in human and animal tissues using Raman spectroscopy. Venkata Ramana Kodati et al. used Raman spectroscopy to identify uric acid-type kidney stones. William Carswell et al. quantified macro- and microhematuria in human urine. According to the above and many more results Raman Spectroscopy can be used to quantify the variations in concentrations of analytes present in urine.

1.5 Aim of the Thesis

The objective of this thesis is to apply Surface-enhanced Raman Spectroscopy (SERS) for the measurement and quantification of unidentified concentrations of urea, uric acid, and creatinine in urine samples. SERS is an advanced analytical technique that combines the principles of Raman spectroscopy with enhanced signal intensities achieved by interacting molecules with specially designed plasmonic nanostructures. The main focus of this research is to collect SERS spectra containing known concentrations of urea, uric acid, and creatinine, and establish calibration curves. These calibration curves will establish a correlation between the SERS signal intensities and the

concentrations of the analytes, enabling the determination of unknown concentrations.

Chapter 2

Materials and Characterization Techniques

2.1 Materials

Pure urea, uric acid, and creatinine were bought from Sigma Aldrich. Urea, uric acid, and creatinine's aqueous solution were prepared in DI (Deionized) water.

The urine of a healthy person contains an average amount of 1639 mg/dl for urea, 104 mg/dl for creatinine, and 34 mg/dl for uric acid [24]. However, for medical diagnosis, the clinically significant levels of urea, uric acid, and creatinine in urine are in the ranges of 900–3000 mg/dl, 16–100 mg/dl, and 50–265 mg/dl, respectively [44]. Samples were prepared at various concentrations within these ranges to facilitate the analysis of changes in the concentrations of these analytes. For the synthesis of gold nanoparticles, chloroauric acid ($\text{HAuCl}_4 \cdot 3\text{H}_2\text{O}$), and tri-sodium citrate ($\text{Na}_3\text{C}_6\text{H}_5\text{O}_7 \cdot 3\text{H}_2\text{O}$) were bought from Sigma Aldrich and Merck Millipore, respectively.

2.2 Synthesis of Gold nanoparticles

Gold nanoparticles were fabricated using Turkevich Method [45]. First, took 10 ml of 1 mM chloroauric acid and boiled it to 100 °C temperature. Additionally, it was stirred simultaneously at a speed of 700 rpm on a magnetic stirrer. When the solution started boiling, then 400 µl of 39 mM tri-sodium citrate was added drop by drop in the solution and stirred continuously till the mixture turned into a wine-red color. When the color of the solution turned into wine red, the heating was turned off. The solution was continuously stirred until it reached the room temperature, change in the color of the solution, indicating the successful formation of gold nanoparticles.

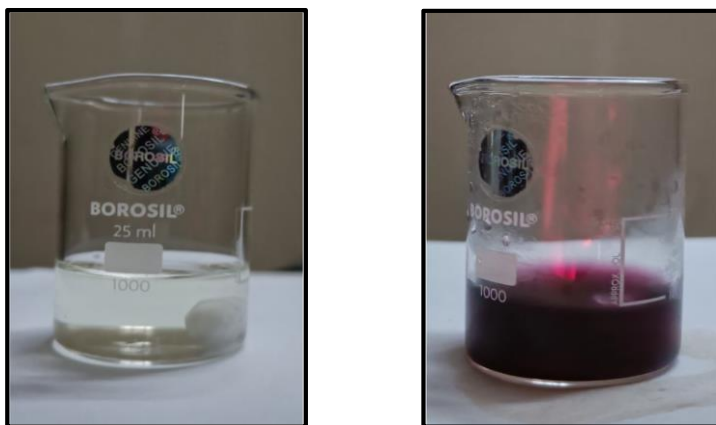


Fig. 2.1: Synthesis of Gold Nanoparticles (Colorless to wine-red color)

2.3 Sample preparation

Pure urea, uric acid, and creatinine powders were taken for sample preparation. Aqueous stock solutions of these were prepared in DI water. The concentration of the stock solution of urea and uric acid is 50 mM, 5 mM and 50 mM, respectively. For getting different concentrations (these concentrations were in accordance with the diagnostically relevant concentration range) dilute these stock solutions with DI water.

The desired concentration of Urea (mM)	Required volume from a stock solution (μL)	The required volume of DI water (μL)
2	40	960
5	100	900
10	200	800
20	400	600
30	600	400
50	1000	0

Table 2.1: Different Urea Concentration in Prepared Samples

The desired concentration of Uric Acid (mM)	Required volume from a stock solution (μL)	The required volume of DI water (μL)
0.25	50	950
0.50	100	900
0.75	150	850
1.00	200	800
2.00	400	600

Table 2.2: Varying Concentrations of uric acid for Analysis

The desired concentration of Creatinine (mM)	Required volume from a stock solution (μL)	The required volume of DI water (μL)
2	40	960
5	100	900
10	200	800
20	400	600
30	600	400

Table 2.3: Prepared different concentrations of creatinine

In the sample preparation process, we made an aqueous solution of urea and uric acid at different concentrations with DI water. Urea concentrations are 2, 5, 10, 20, 30, and 50 mM and uric acid concentrations are 0.25, 0.50, 0.75, 1.0, and 2.0 mM while creatinine concentrations are 2, 5, 10, 20, and 30 mM. In this work, Gold Nanoparticles (GNPs) were employed as the substrate, and the sample preparation involved combining 5 μL of GNPs with 5 μL of aqueous solutions containing different concentrations of urea, uric acid, and creatinine. Mix thoroughly this mixture and place two drops of 5 μL each on glass slides from each sample. Then, the drops were left to dry naturally at room temperature, and once they were completely dried, we obtained their Raman spectra from three different points along the circumference of each drop.

2.4 Characterization Techniques

For the characterization of synthesized gold nanoparticles, following characterization techniques such as UV-vis absorption spectroscopy, scanning electron microscopy, and transmission electron microscopy, were used. Further, bio-analytes were investigated using surface-enhanced Raman spectroscopy for reliable disease diagnosis. Instrumentation is as following described.

2.4.1 UV-Vis Absorption Spectroscopy

UV-vis spectroscopy is a type of spectroscopic method which quantifies the amount of specific UV or visible light wavelengths that are absorbed by or transmitted through a substance in comparison to a reference or blank sample.

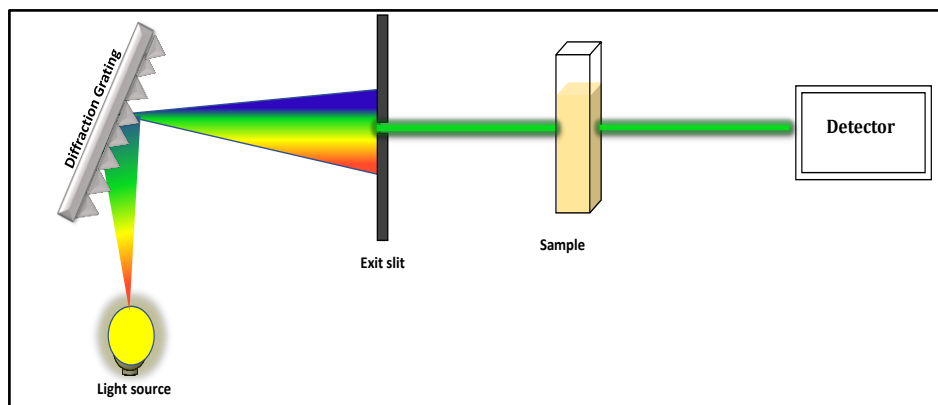


Fig. 2.2: Schematic representation of absorption spectroscopy

A spectrophotometer is used to measure the amount of light absorbed by a sample at a specific wavelength. A spectrophotometer contains a light source that emits light with a wide range of wavelengths. Then light passes through a monochromator which chooses a narrow spectrum of wavelengths that are directed towards the sample. Generally, it includes a diffraction grating or prism that separates the light into its individual wavelengths. The monochromatic light is then directed toward the sample cell. The sample cell is a small rectangular or cylindrical container made up of quartz or glass that contains sample for measurements. Light passes through sample cell and detected by detector which can be photo diode or photo multiplier tube (PMT).

When light passes through a sample, its intensity is compared to the intensity of light before passing through the sample and this intensity difference is used to calculate the amount of absorbed light. According to the Beer-Lambert law, amount of light that is absorbed by sample is directly proportional to the concentration of sample and path length (which is usually standardized to 1 cm) of sample cell.

$$\text{Absorbance } A = \log \left(\frac{I_0}{I_T} \right) = \epsilon \cdot d \cdot c$$

Where I_0 and I_T are incident and transmitted intensity respectively, ϵ is the absorption coefficient, d is the path length (in cm) of the sample solution, and c (in M) is the concentration of the sample solution.

2.4.2 Scanning Electron Microscopy (SEM)

Scanning electron microscope is a powerful and effective imaging technique that allows for the imaging of surfaces with high resolution. The fundamental concept of the SEM process is the interaction of a high-energy electron beam with a sample, which results in secondary electrons and other signals that can be detected and used to build an image. The sample is mounted on a moving stage within the SEM chamber, which is then pumped to a high vacuum to avoid the scattering of electrons with air molecules. Then the sample is illuminated by a beam of highly-energized electrons and focused on the sample using a series of electromagnetic lenses.

When an electron beam strikes the sample, many kinds of signals, including secondary electrons, backscattered electrons, and X-rays, are generated. Secondary electrons are low-energy electrons and are generated when highly-energized electrons strike sample's surface. Using these electrons, SEM image is created, which gives information about morphology of sample's surface. Backscattered are high-energy electrons that are scattered back from the sample's surface. These electrons give information about sample's composition and density. X-rays are produced when the high-energy electrons in the sample collide with the atoms of sample, making it a possible to analyze the sample's elements. This technique is frequently used in materials science, nanotechnology, and biology to investigate the nanoscale structure and characteristics of materials. It is very helpful for analyzing the composition, particle size, and surface morphology of materials.

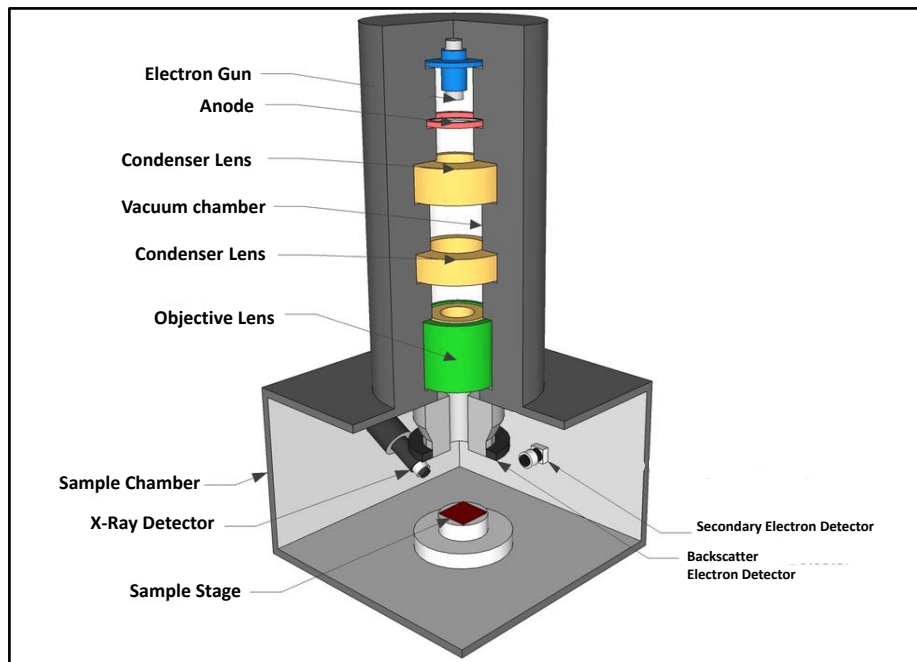


Fig. 2.3: Scanning Electron Microscope (SEM)

2.4.3 Transmission Electron Microscope (TEM)

Transmission electron microscopy (TEM) is a powerful imaging tool that uses an electron beam to provide the composition and structure of the sample. The basic concept behind TEM is to send an electron beam through a thin sample and then detect the electrons that pass through the sample to produce an image.

A sample for TEM imaging is prepared by cutting it into thin sections, usually less than 100 nm thick. The TEM column is loaded with a thin support film on which a thin sample is mounted. With the help of an electron gun, highly energized electrons are created and directed at the sample by a series of electromagnetic lenses including a condenser lens and objective lens, which also accelerate the beam of electrons. Through the thin sample, the electron beam is transmitted. The transmitted electrons through the sample are refocused. By using these electrons, an image of the sample is created, and using a projector lens these images are magnified and can be viewed on a screen and recorded digitally.

TEM is used in a wide range of scientific fields, including materials science, biology, nanotechnology, forensics analysis, chemistry, and physics to provide high-resolution images and gives topographical,

morphological, and compositional information about sample at the nanoscale level.

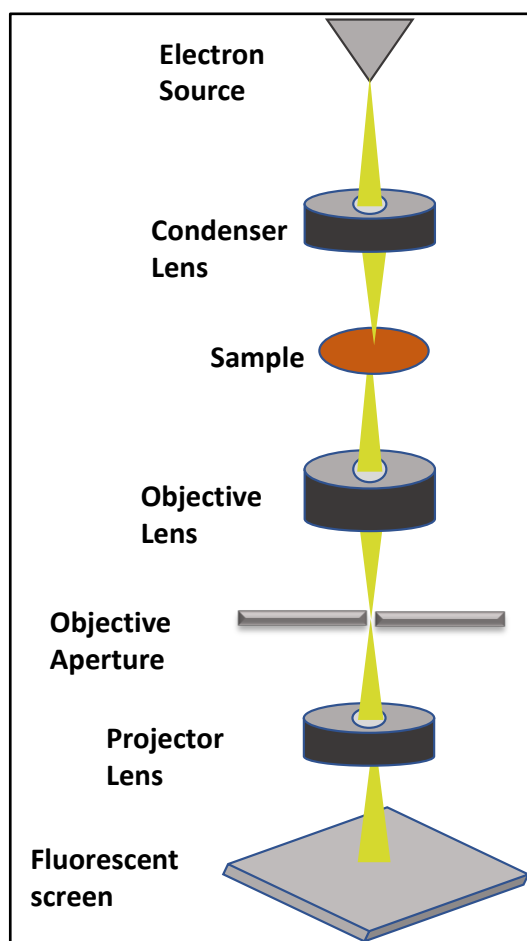


Fig. 2.4: Ray diagram of Transmission Electron Microscope (TEM)

2.4.4 Raman Spectroscopy

Using a Raman spectroscopy setup, the Raman spectra of urea, uric acid, and creatinine were obtained. The schematic representation of Raman spectroscopy is as shown below figure.

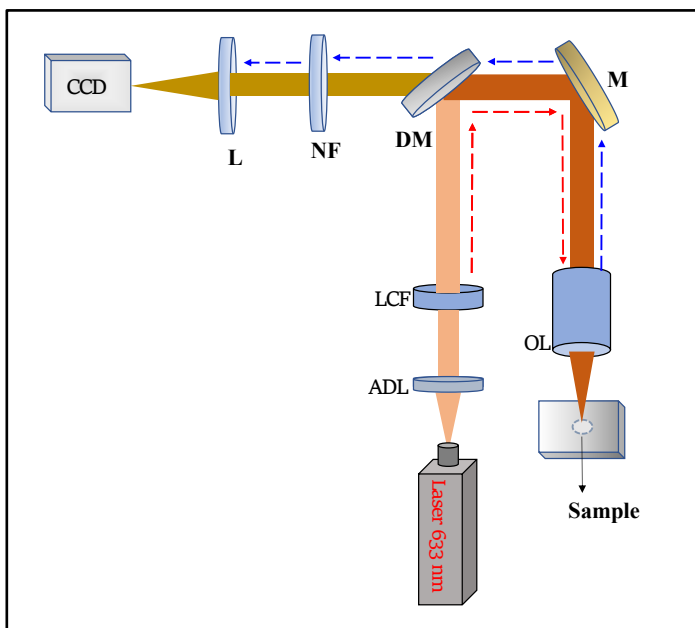


Fig. 2.5: Raman instrumentation where the expanded form is ADL- achromatic doublet lens; LCF- laser clean-up filter; DM- dichroic mirror; M- plane mirror; OL- objective lens; NF- notch filter; CCD- charge-coupled device

The excitation source is a 633 nm single-mode diode laser. Using a 50 mm achromatic doublet lens (ADL), the laser beam is first collimated. The collimated beam is next filtered with a bandpass or laser clean-up filter (LCF) and then reflected by a dichroic mirror (DM) which is kept at a 45° angle. For directing the beam toward the sample, another mirror (M) is positioned at a 45° angle. Using a microscope objective lens (OL), the excitation laser beam is focused on the sample's surface. The same objective lens is used to collect the sample's backscattered Raman signal, which is then reflected by M and transmitted by DM. Then the Raman signal is processed through a notch filter (NF) where elastically scattered Rayleigh components are removed. A convex lens (L) was also used for combining the Raman signal at the entry slit of an imaging spectrograph fitted with a charge-coupled device (CCD) camera.

2.5 Quantitative Estimation of Analytes

To predict unknown concentrations, we followed a specific methodology. Initially, we collected a comprehensive dataset of known concentrations of urea, uric acid, and creatinine and their corresponding

intensities. Next, we made an intensity vs. concentrations calibration plot for these analytes. Following this, we performed linear regression analysis and checked the accuracy and goodness of fit of the regression model. Through the regression analysis, the coefficients a (intercept) and b (slope) in the equation $y = a + b \cdot x$ were estimated. The performance of the model was evaluated using R-squared, which provide insights into the accuracy and goodness of fit of the regression model.

By following this methodology, we successfully predicted unknown concentrations by substituting the intensities of the unknown samples into the linear regression equation $y=a+b \cdot x$. The unknown concentrations estimated varied from prepared unknown concentrations in the range of 10-15%.

Chapter 3

Results and Discussion

For the experiment, the varying concentrations of urea, uric acid, and creatinine in the aqueous solutions are from 2 mM to 50 mM, 0.25 mM to 2.00 mM, and 2 mM to 30 mM, respectively.

To prepare these samples, a mixture was created by combining 5 μ l of gold nanoparticles (GNPs) with 5 μ l of aqueous solutions of analyte of different concentrations. Gold Nanoparticles were synthesized using the Turkevich method. Firstly, prepared Gold Nanoparticles (GNPs) were observed by UV-Vis Absorbance spectroscopy. Figure 3.1 shows the absorption spectrum of GNPs, which shows the absorption maxima at 530 nm and the estimated size of GNPs could be around 30 nm.

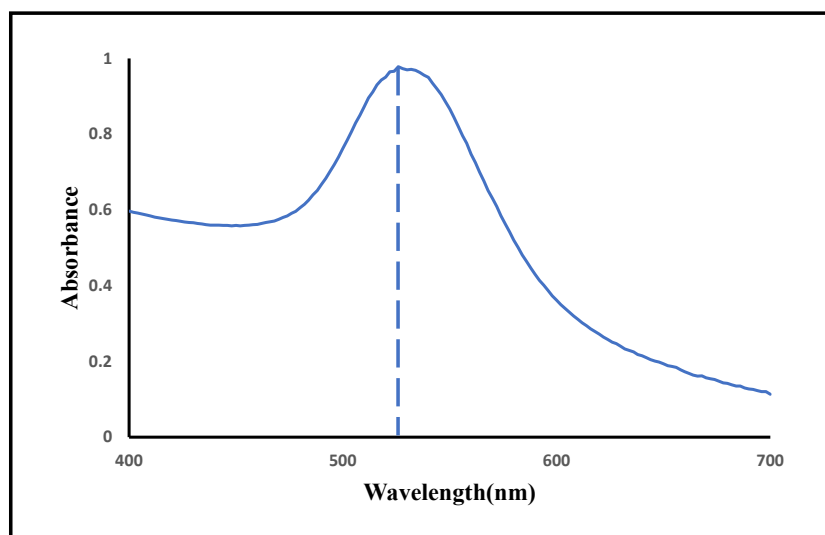


Fig. 3.1: UV-vis absorbance spectrum of the synthesized GNPs

For confirming the size of GNPs Scanning Electron Microscopy (SEM) and Transmission Electron Microscopy (TEM) images were acquired. The mean diameter of synthesized GNPs was observed around 30 nm.

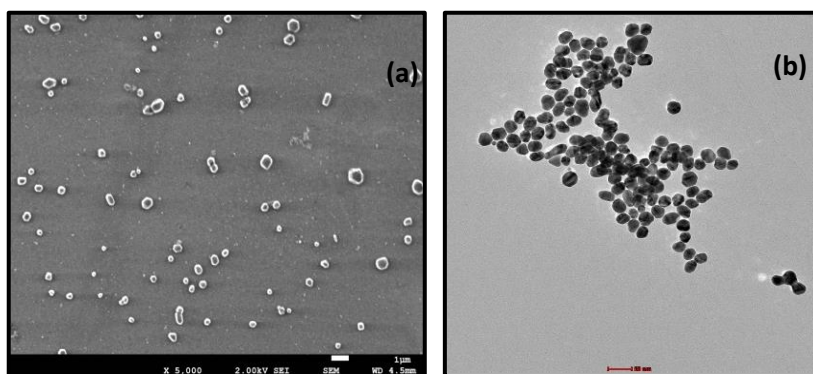


Fig. 3.2: (a) SEM and (b) TEM image of GNPs and the size of GNPs were around 30 nm.

To investigate the Raman spectra of urea, uric acid, and creatinine using SERS, a liquid sample was prepared by creating a drop consisting of a mixed solution of gold nanoparticles and a specific concentration of the analyte. Then, this drop was deposited onto an aluminum foil and let it dry at the room temperature. Once it was completely dried, its Raman spectrum was obtained.

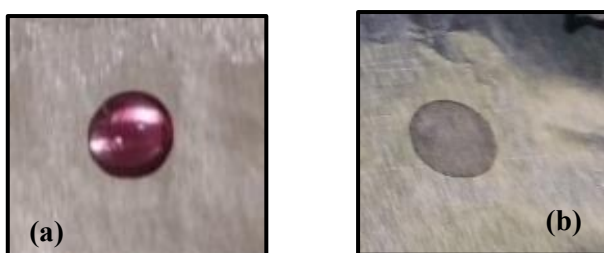


Fig. 3.3: (a) Liquid and (b) Dried drop containing GNPs and analyte

To study the effects of varying analyte concentrations, experiments were conducted by preparing different concentrations of these analytes with GNPs and Raman spectra were collected from them. The obtained Raman spectra for urea, uric acid, and creatinine at various concentrations were further utilized to prepare calibration curves, which provide a quantitative relationship between the Raman signal intensity at the characteristic peak and the corresponding analyte concentration.

Figure 3.4 displays the Raman Spectrum of urea at different concentrations. Two prominent peaks are observed at 997 cm^{-1} and 1160 cm^{-1} and these are attributed to the N-C-N stretching vibrational mode and NH_2 rocking vibrational mode, respectively. These peaks provide valuable insights into the molecular vibrations and

structural characteristics of urea [41]. This vibrational information can be effectively utilized for the identification and analysis of urea in various samples, thereby enabling its detection and quantification, even in unknown concentrations.

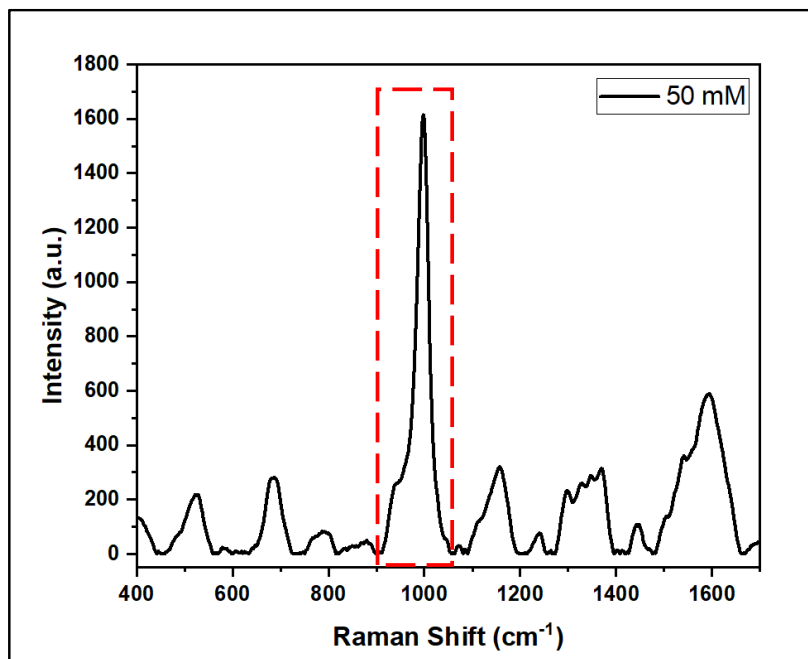


Fig. 3.4: The Raman spectrum of urea at 50 mM concentration measured from the dried-up liquid drop.

The peak around 997 cm⁻¹ is the most prominent peak for urea and was chosen for quantification of urea because it shows a linear variation in Raman intensity with concentration. Figure 3.5 shows Raman spectra for all different known concentrations of urea at 997 cm⁻¹.

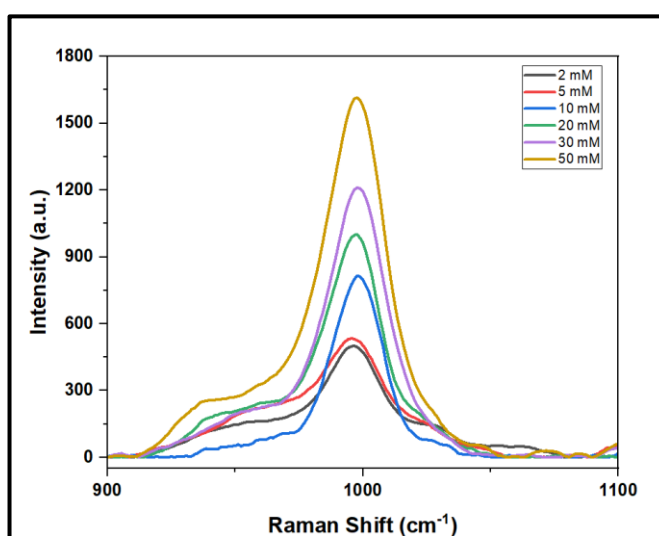


Fig. 3.5: Raman spectrum of urea at 997 cm⁻¹

Figure 3.6 presents the Raman Spectrum of uric acid at different concentrations. Five prominent peaks are observed at 495 cm^{-1} , 641 cm^{-1} , 1027 cm^{-1} , 1405 cm^{-1} , and 1658 cm^{-1} attributed to C-N-C vibrations, ring breathing mode, C-N stretching, N-C-C stretching, and C=O stretching, respectively [42].

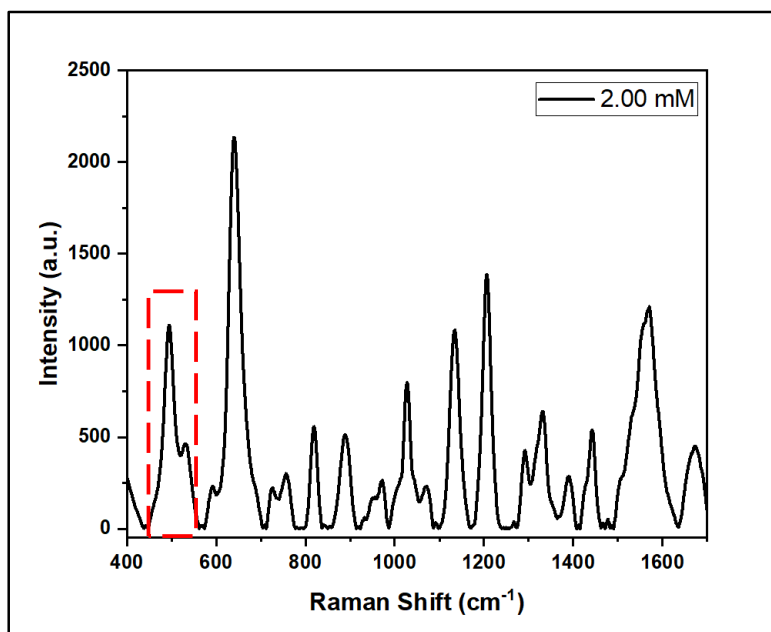


Fig. 3.6: The Raman spectrum of uric acid at 2.0 mM concentrations measured from the dried-up liquid drop.

The most prominent peak observed at 495 cm^{-1} in the Raman spectra corresponds to uric acid and has been selected for the quantification of urea. Figure 3.7 shows the Raman spectra for various known concentrations of uric acid specifically at 495 cm^{-1} .

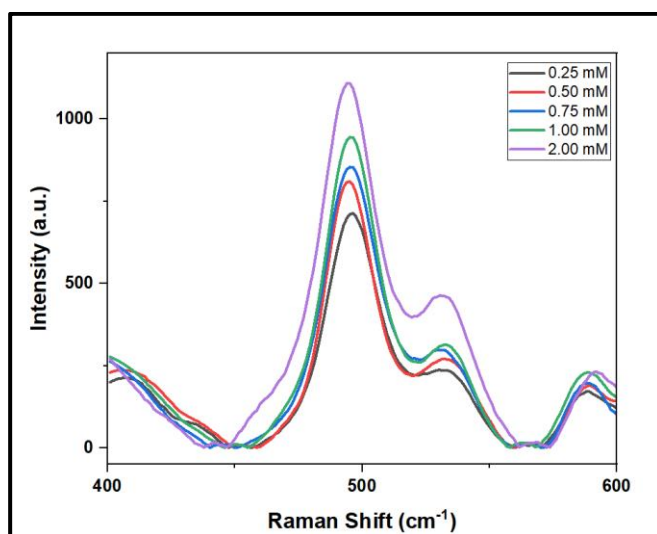


Fig. 3.7: Raman spectrum of uric acid at 495 cm^{-1}

In figure 3.8, the Raman spectrum of creatinine is presented, showing its variation at different concentrations. The spectra exhibit four distinct Raman peaks at 601 cm^{-1} , 683 cm^{-1} , 840 cm^{-1} , and 908 cm^{-1} . Specifically, the 601 cm^{-1} peak corresponds to C=O deformation, N-CH₃ stretching, and ring vibrations. The 683 cm^{-1} peak represents C-NH₂ and C=O stretching, as well as ring vibrations. Similarly, the 840 cm^{-1} peak indicates C-NH₂ deformation and ring vibrations, while the 908 cm^{-1} peak signifies C-C-N stretching [43].

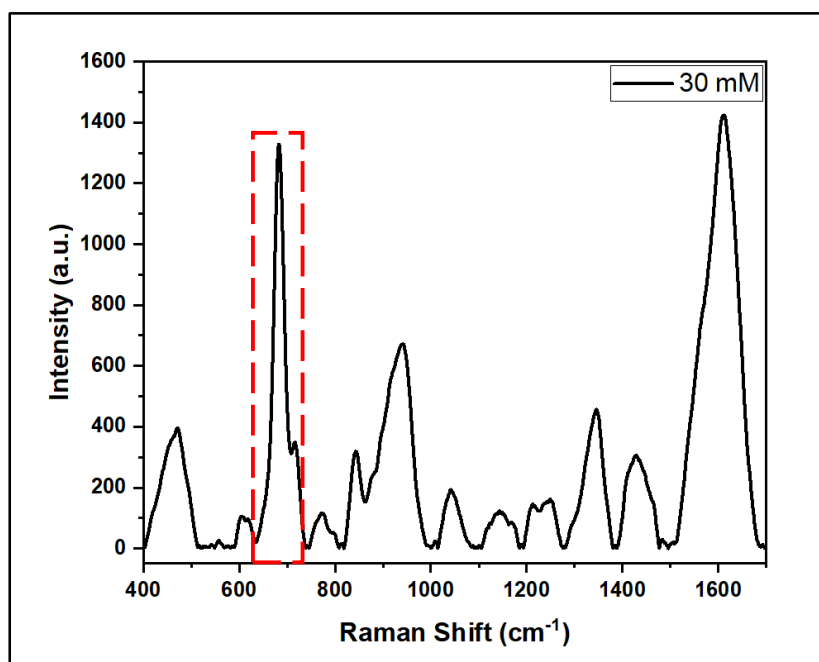


Fig. 3.8: The Raman spectrum of creatinine at the concentrations 30 mM measured from the dried-up liquid drop.

The peak observed at 683 cm^{-1} in the Raman spectra is the primary peak for creatinine and has been selected for the quantification of creatinine due to its linear relationship with concentration. Figure 3.9 presents the Raman spectra for various known concentrations of urea specifically at 683 cm^{-1} .

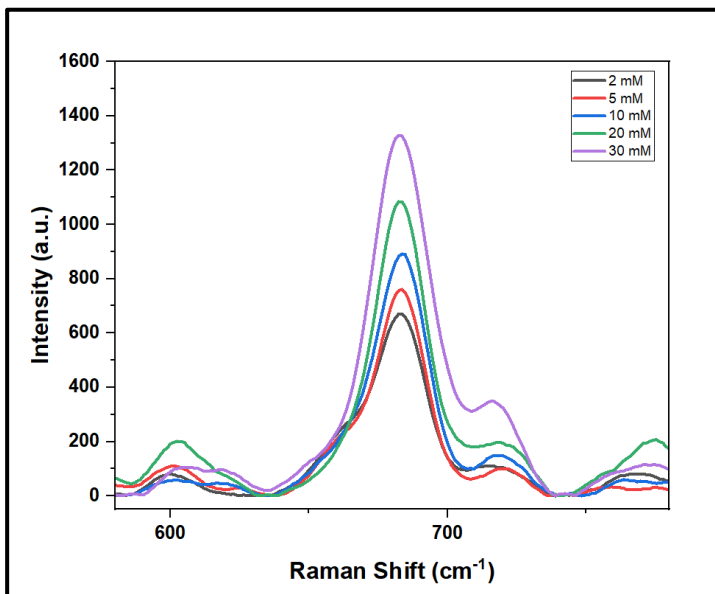


Fig. 3.9: Raman spectra for creatinine at different known concentration at 683 cm^{-1} .

The Raman spectra of urea, uric acid, and creatinine at different concentrations revealed concentration-dependent changes in Raman intensity. The observed variations allowed for the construction of a calibration curve, enabling the estimation of these analyte concentrations in unknown samples based on their Raman spectra. For constructing the calibration curve, a characteristic peak is selected. This peak is chosen to ensure that the relationship between the peak intensity and the concentration of the analyte follows a linear fashion. This enables us to accurately determine the concentration of the analyte in unknown samples by comparing their Raman peak intensities to the calibration curve.

In Figure 3.10, the calibration curve for urea is presented, illustrating the relationship between the Raman peak intensity and the corresponding concentrations of the analyte at 997 cm^{-1} . The curve exhibits a strong correlation between Raman intensity and concentrations, as indicated by its high R^2 value of 0.98. The known concentrations are on the x-axis and the corresponding Raman peak intensities on the y-axis.

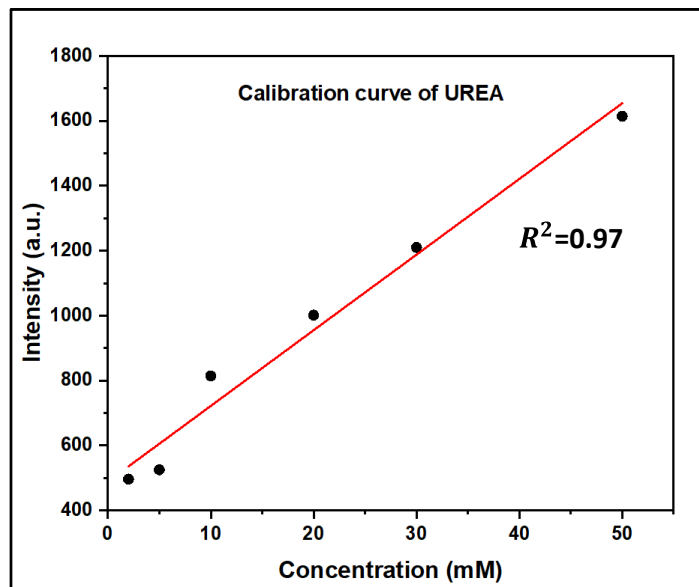


Fig. 3.10: Calibration curve depicting the relationship between the Raman peak intensity and the concentrations of urea.

The calibration curve for uric acid, as represented in Figure 3.11, demonstrates the relationship between the Raman peak intensity at 495 cm^{-1} and the corresponding concentrations of the analyte. The R^2 value for calibration curve of uric acid is 0.96 that indicates its high accuracy and reliability.

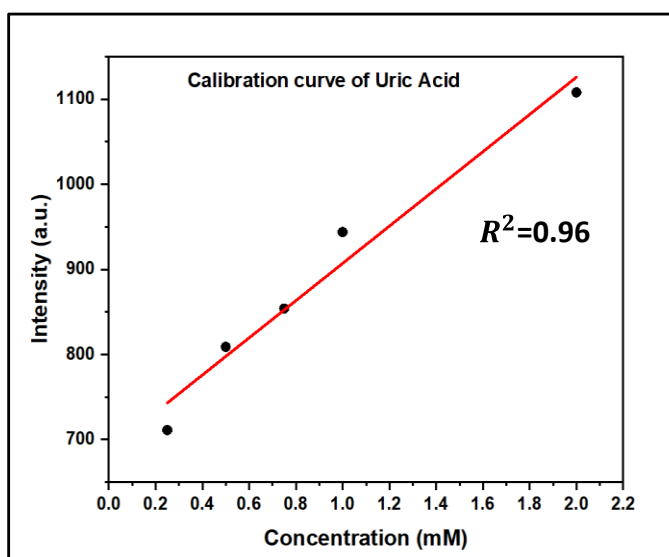


Fig. 3.11: Correlation between Raman Intensity and Uric Acid Concentrations

Similarly, for creatinine, the calibration curve (Figure 3.12) demonstrates a strong relationship between the Raman peak intensity at 683 cm^{-1} and the concentrations of creatinine. The R^2 value obtained

for the calibration curve is 0.99, indicating a high level of accuracy and precision.

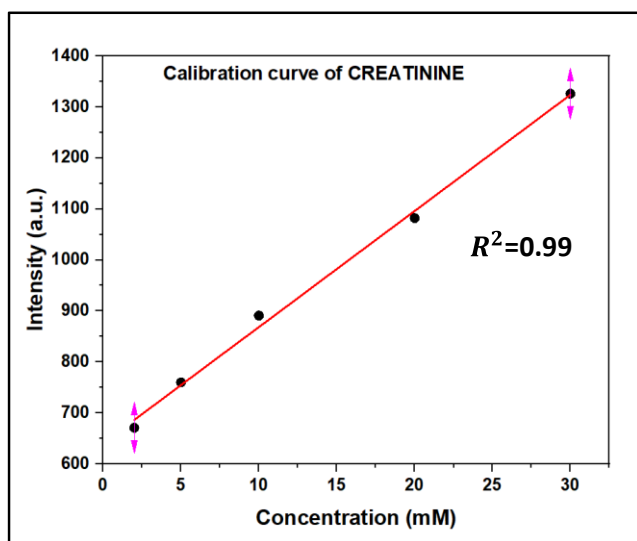


Fig. 3.12: Calibration Curve Analysis for Creatinine Concentrations

The unknown concentration samples of urea, uric acid, and creatinine were analysed using Surface-enhanced Raman Spectroscopy (SERS) to determine their concentrations. Raman spectra were acquired for each unknown sample, following the same experimental setup as the known concentration samples. The obtained Raman spectra exhibited distinctive Raman peaks associated with the analytes, enabling their identification and quantification. Figure 3.13, 3.14, and 3.15 displays the Raman spectra obtained from the unknown concentration samples.

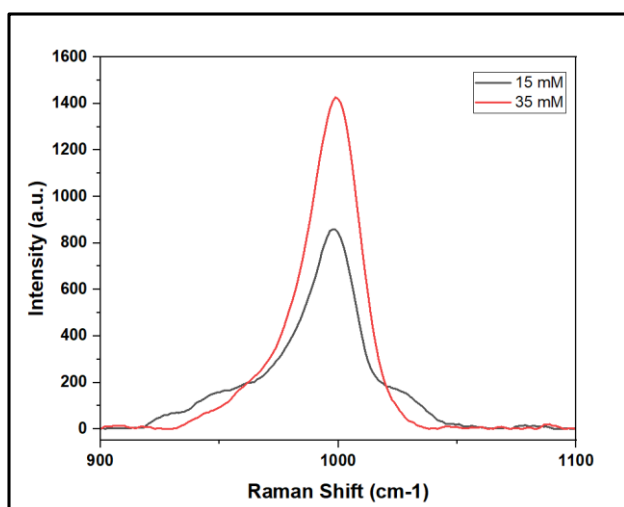


Fig. 3.13: Raman spectrum of the unknown concentrations of urea

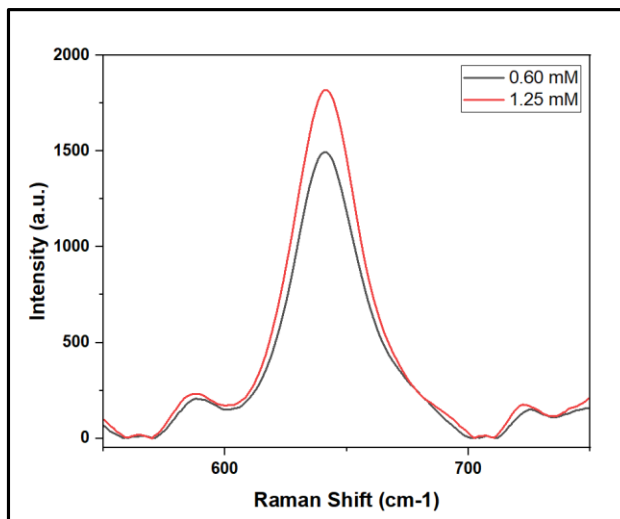


Fig. 3.14: Raman spectrum of the unknown concentrations of uric acid

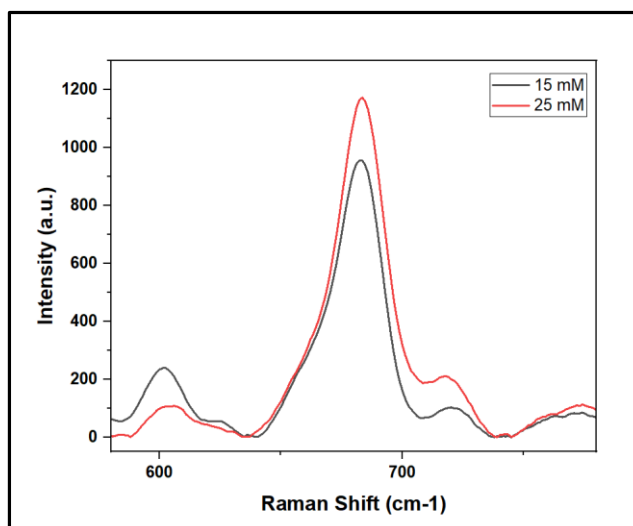


Fig. 3.15: Raman spectrum of the unknown concentrations of creatinine

By comparing the unknown sample Raman spectra to the calibration curves established using known concentrations, we determined the concentrations of urea, uric acid, and creatinine in the respective unknown samples. In this case, the unknown concentrations for urea sample were found to be 17.29 mM and 40.08 mM, which deviated slightly from the original concentrations of 15 mM and 35 mM with an error value of 10-15%. In the case of uric acid sample, the analysis of unknown concentrations revealed values of 0.67 mM and 1.23 mM, which showed a slight deviation from the original concentrations of 0.60 mM and 1.25 mM with an error value of 10-15% when quantified using the calibration curve. And, in the case of creatinine sample, the

quantification of unknown concentrations resulted in values of 14.27 mM and 24.13 mM, which showed a slight deviation from the original concentrations of 15 mM and 25 mM with an error value of 5-6%. These deviations indicate a minor difference between the measured and expected concentrations. However, considering the associated uncertainty or error range of 10-15%, these values fall within an acceptable accuracy range.

Chapter 4

Conclusion and Future Prospect

4.1 Conclusion

This thesis presents a comprehensive quantitative and qualitative investigation of urea, uric acid, and creatinine using Surface-enhanced Raman Spectroscopy as a powerful analytical technique. The study successfully constructed calibration curve for each analyte stabilizing a strong correlation between Raman peak intensities and concentrations. The obtained R^2 values of 0.98 for urea, 0.99 for uric acid, and 0.99 for creatinine demonstrate the accuracy and the reliability of the calibration method.

Furthermore, unknown concentrations of urea, uric acid, and creatinine were determined using the calibration curve. The obtained results closely matched the expected concentrations, although with slight deviations. The accuracy of quantification process was supported by the small error range within 10-15%. These findings highlight that Raman spectroscopy might emerge as a reliable method for analysis and quantification of urine. The implications of this project are significant in various fields. In the field of clinical diagnostics, the accurate quantification of urea, uric acid, and creatinine can assist in the assessment of kidney functions and the diagnosis of related disorders. In biomedical research, the ability to quantify these analytes provide valuable information for studying metabolic process and disease mechanism.

4.2 Future Prospect

Progress in miniaturization and the advancement of portable Raman spectrometers have the potential to revolutionize point-of-care applications, allowing for on-site analysis and real-time monitoring in various clinical and field environments. The exploration of strategies for miniaturization and the engineering of compact devices will play a crucial role in making Raman spectroscopy practical and accessible for routine analysis. In further studies, there can be an evaluation of the potential of this technique in analyzing different types of bodily fluids.

It's utilization in clinical settings for the purpose of rapid and precise disease diagnosis can be explored.

References

1. Doria A., Zen M., Canova M., Bettio S., Bassi N., Nalotto L., Rampudda M., Ghirardello A., Iaccarino L. (2010) “SLE diagnosis and treatment: when early is early”, *Autoimmun* 10(1):55-60.
<https://doi.org/10.1016/j.autrev.2010.08.014>
2. Sandra L., Hui H., Marvin Z., “Early detection of disease and scheduling of screening examination”, *Statistical methods in medical research*, <https://doi.org/10.1191/0962280204sm377ra>
3. McEwen C. N., McKay R. G., Larsen B. S., (2005) “Analysis of solids, liquids, and biological tissues using solids probe introduction at atmospheric pressure on commercial LC/MS instruments”. *Analytical Chemical*, PMID: 16316194.
4. Vaught J. B., Henderson M. K., (2011) “Biological sample collection, processing, storage and information management”, *IARC Sci Publ.*, PMID: 22997855.
5. Badiie P., (2013) “Evaluation of human body fluids for the diagnosis of fungal infections”, *Biomed Res Int.* 2013;2013:698325. <https://doi.org/10.1155/2013/698325>
6. Pettersson Bergstrand M., Beck O., Helander A. (2018), “Urine analysis of 28 designer benzodiazepines by liquid chromatography–high-resolution mass spectrometry”, *Clinical Mass Spectrometry*, (<https://doi.org/10.1016/j.clinms.2018.08.004>)
7. Penders J., Fiers T., Delanghe J. R. (2002), “Quantitative Evaluation of Urinalysis Test Strips”, *Clinical Chemistry*, 48, 2236
8. Khristenko N., Domon B. (2015), “Quantification of proteins in urine samples using targeted mass spectrometry methods”, *Clinical Proteomics*, 207-220
9. Armstrong J. A., (2007) “Urinalysis in Western culture: a brief history”, *Kidney Int.*, (<https://doi.org/10.1038/sj.ki.5002057>)

10. Tuuminen T., “Urine as a specimen to diagnose infections in twenty-first century: focus on analytical accuracy”, *Front Immunol.* (<https://doi.org/10.3389/fimmu.2012.00045>)
11. Connor H. (2001) “Medieval uroscopy and its representation on misericords--part 1: Uroscopy” *Clin Med (London)*. Nov-Dec;1(6):507-9. (<https://doi.org/10.7861/clinmedicine.1-6-507>)
12. Mozolowski W., (1948) “Chemical composition of normal urine”, *Lancet.*;1(6498):423.
([https://doi.org/10.1016/s0140-6736\(48\)90292-x](https://doi.org/10.1016/s0140-6736(48)90292-x))
13. Putnam D. F. (1971), “Composition and concentrative properties of human urine”
14. Piech T. L.Wycislo K. L. (2019), “Importance of Urinalysis”, *Veterinary Clinics of North America: Small Animal Practice*, 49, 233-245 (<https://doi.org/10.1016/j.cvsm.2018.10.005>)
15. Echeverry G, Hortin GL, Rai AJ. (2010) “Introduction to urinalysis: historical perspectives and clinical application”. *Methods Mol Biol.*; https://doi.org/10.1007/978-1-60761-711-2_1
16. Walker A. B., “The importance of urine analysis in diagnosis” *JAMA*. 1895; XXIV (4):122–123.
(<https://doi.org/10.1001/jama.1895>)
17. Chekmeneva E, Dos Santos Correia G, Gómez-Romero M, Stamler J, Chan Q, Elliott P, Nicholson JK, Holmes E. (2018) “Ultra-Performance Liquid Chromatography-High-Resolution Mass Spectrometry and Direct Infusion-High-Resolution Mass Spectrometry for Combined Exploratory and Targeted Metabolic Profiling of Human Urine”. *J Proteome Res.* <https://doi.org/10.1021/acs.jproteome.8b00413>
18. Khamis MM, Adamko DJ, El-Aneed A. (2017) “Mass spectrometric based approaches in urine metabolomics and biomarker discovery” *Mass Spectrom Rev. Mar*;36(2):115-134.
(<https://doi.org/10.1002/mas.21455>)
19. Khamis M. M., Adamko D. J.El-Aneed A. (2017), “Mass spectrometric based approaches in urine metabolomics and

- biomarker discovery”, *Mass Spectrometry Reviews*, 36, 115-134 (<https://doi.org/10.1002/mas.21455>)
20. Suryavanshi, M. V., S. D. Jadhav, R. P. Gune, M. S. Bhatia, and Y. S. Shouche. “HPLC ANALYSIS OF HUMAN URINE FOR OXALATE CONTENT”. *International Journal of Pharmacy and Pharmaceutical Sciences*, vol. 8, no. 12, Dec. 2016, pp. 54-59, <https://doi.org/10.22159/ijpps.2016v8i12.13168>
 21. Hampe MH, Panaskar SN, Yadav AA, Ingale PW. (2017) “Gas chromatography/mass spectrometry-based urine metabolome study in children for inborn errors of metabolism: An Indian experience”, *Clin Biochem.*;50(3):121-126. <https://doi.org/10.1016/j.clinbiochem.2016.10.015>
 22. Liu X, et al “Characterization of LC-MS based urine metabolomics in healthy children and adults”, *PeerJ*. 2022 Jun 22;10: e13545. <https://doi.org/10.7717/peerj.13545>
 23. Kumps A., Duez P., Genin J.Mardens Y. (1999), “Gas Chromatography–Mass Spectrometry Analysis of Organic Acids: Altered Quantitative Response for Aqueous Calibrators and Dilute Urine Specimens”, *Clinical Chemistry*, 45, 1297
 24. Premasiri WR, Clarke RH, Womble ME. (2001) “Urine analysis by laser Raman spectroscopy”, *Lasers Surg Med.*;28(4):330-4. <https://doi.org/10.1002/lsm.1058>
 25. Kiviat N. B.Critchlow C. W. (2002), “Novel Approaches to Identification of Biomarkers for Detection of Early Stage Cancer”, *Disease Markers*, 18, (<https://doi.org/10.1155/2002/589075>)
 26. Dutta, Surjendu Bikash. "Optical spectroscopy-based urine analysis for disease diagnosis." (2020).
 27. Penner, Michael H. (2010), “Basic principles of spectroscopy”, https://doi.org/10.1007/978-1-4419-1478-1_21
 28. Achetib, N., Falkena, K., Swayambhu, M. *et al.* (2023) “Specific fluorescent signatures for body fluid identification

using fluorescence spectroscopy”, *Sci Rep* 13, 3195
<https://doi.org/10.1038/s41598-023-30241-7>

29. Brown JQ, Vishwanath K, Palmer GM, Ramanujam N., (2009) “Advances in quantitative UV-visible spectroscopy for clinical and pre-clinical application in cancer”, *Curr Opin Biotechnol.*;20(1):119-31.
<https://doi.org/10.1016/j.copbio.2009.02.004>
30. Graves P.Gardiner D. (1989), “Practical Raman spectroscopy, Springer”
31. Mitsutake H., Ronei J., Breitzkreitz C., (2019) “Raman Imaging Spectroscopy: History, Fundamentals and Current Scenario of the Technique”, *J. Braz. Chem. Soc.* 30 (11)
32. Leordean C., Canpean V.Astilean S. (2012), “Surface-Enhanced Raman Scattering (SERS) Analysis of Urea Trace in Urine, Fingerprint, and Tear Samples”, *Spectroscopy Letters*, 45, 550-555 (<https://doi.org/10.1080/00387010.2011.649439>)
33. Zong, C., Xu, M., Xu, L. J., Wei, T., Ma, X., Zheng, X. S., ... & Ren, B. (2018). “Surface-enhanced Raman spectroscopy for bioanalysis: reliability and challenges”, *Chemical reviews*, 118(10), 4946-4980
34. José A. Sánchez-Gil, José V. García-Ramos, and Eugenio R. Méndez, "Electromagnetic mechanism in surface-enhanced Raman scattering from Gaussian-correlated randomly rough metal substrates," *Opt. Express* 10, 879-886 (2002)
35. Kim J, Jang Y, Kim NJ, Kim H, Yi GC, Shin Y, Kim MH, Yoon S. (2019) “Study of Chemical Enhancement Mechanism in Non-plasmonic Surface Enhanced Raman Spectroscopy (SERS)”, *Front Chem.*; 7:582.
<https://doi.org/10.3389/fchem.2019.00582>

36. S.B. Dutta et al, (2019) "Nano-trap Enhanced Raman Spectroscopy: An Efficient Technique for Trace Detection of Bio analytes", *Analytical Chemistry*, 91, 5, 3555-3560.
37. Deegan R. D., Bakajin O., Dupont T. F., Huber G., Nagel S. R. Witten T. A. (1997), "Capillary flow as the cause of ring stains from dried liquid drops", *Nature*, 389, 827-829 (<https://doi.org/10.1038/39827>)
38. S. B. Dutta et al, "Drop-Coating Deposition Raman Spectroscopy (DCDRS) for Quantitative Detection of Urinary Creatinine: A feasibility study", *Laser Physics-IOP Science*.
39. de Sousa Vieira EE, (2017) "Biochemical Analysis of Urine Samples from Diabetic and Hypertensive Patients without Renal Dysfunction Using Spectrophotometry and Raman Spectroscopy Techniques Aiming Classification and Diagnosis", *Bioengineering (Basel)*.;9(10):500. <https://doi.org/10.3390/bioengineering9100500>
40. Canetta E, Mazilu M, De Luca AC, Carruthers AE, Dholakia K, Neilson S, Sargeant H, Briscoe T, Herrington CS, Riches AC. (2011) "Modulated Raman spectroscopy for enhanced identification of bladder tumor cells in urine samples", *J Biomed Opt.*;16(3):037002. <https://doi.org/10.1117/1.3556722>
41. Ren M, Arnold MA., (2007) "Comparison of multivariate calibration models for glucose, urea, and lactate from near-infrared and Raman spectra" *Anal Bioanal Chem.*; 387(3):879-88. <https://doi.org/10.1007/s00216-006-1047-4>
42. Tian, F.; Carvalho, et al., "Surface-Enhanced Raman Analysis of Uric Acid and Hypoxanthine Analysis in Fractionated Bodily Fluids", *Nanomaterials* **2023**,1216, <https://doi.org/10.3390/nano13071216>

43. McMurdy JW 3rd, Berger AJ. (2003) “Raman spectroscopy-based creatinine measurement in urine samples from a multi-patient population”, *Applied Spectroscopy*, <https://doi.org/10.1366/000370203321666533>
44. Yu K.-H., Luo S.-F., Tsai W.-P.Huang Y.-Y. (2004), “Intermittent elevation of serum urate and 24-hour urinary uric acid excretion”, *Rheumatology*, 43, 1541-1545
45. Herizchi R, Abbasi E, Milani M, Akbarzadeh A. (2016) “Current methods for synthesis of gold nanoparticles”, *Artif Cells Nanomed Biotechnology*; <https://doi.org/10.3109/21691401.2014.971807>